Lab on a Chip

COMMUNICATION

Paper-based *in-vitro* model for on-chip investigation of the human respiratory system

Rahim Rahimi,[ab] Su Su Htwe,[c] Manuel Ochoa, [ab] Amy Donaldson, [c] Michael Zieger,[d] Rajiv Sood, [d] Ali Tamayol, [ef] Ali Khademhosseini, [efgh] Amir Ghaemmaghami, [c] and Babak Ziaie [*ab]

Received 00th January 20xx,

Accepted 00th January 20xx

DOI: 10.1039/x0xx00000x

www.rsc.org/

Culturing cells at air-liquid interface (ALI) is essential for creating functional *in-vitro* models of lung tissue. We present the use of direct-patterned laser-treated hydrophobic paper as an effective semi-permeable membrane, ideal for ALI cell culture. The surface properties of the paper is modified through selective CO_2 laser-assisted treatment to create a unique porous substrate with hydrophilic regions that regulates fluid diffusion and cell attachment. To select the appropriate model, four promising hydrophobic films were compared with each other in terms of gas permeability and long-term strength in aqueous environment (wet-strength). Among the investigated substrates, parchment paper showed the fastest rate of oxygen permeability (3 times more than conventional transwell cell culture membranes), with the least variation in its dry and wet tensile strength (124 MPa and 58 MPa, remaining unchanged after 7 days of submersion in PBS). The final paper based platform provides an ideal, robust, and inexpensive device for generating monolayers of lung epithelial cells on-chip in a high-throughput fashion for disease modelling and *in-vitro* drug testing.

Introduction

Respiratory epithelium (e.g., the lining of the lungs) is a highly-specialized vital tissue in mammals, serving as the interface between air and internal milieu (blood)[1,2], Fig. 1(a). Under normal conditions, this tissue exhibits remarkable multi-functional properties by providing a physical barrier to protect against pathogens and a medium for rapid (high flux) gas exchange, all while remaining strong and flexible. However, exposure to insults such as hazardous substances, allergens, pathogens, and smoking can alter the integrity of the epithelial cells, resulting in severely impaired respiratory function, which may lead to many life threatening respiratory diseases (e.g., viral respiratory tract infections, asthma, chronic obstructive pulmonary disease, and pneumonia)[3]. Treatment for these conditions is challenging, primarily due to an incomplete understanding of the disease etiologies and the fundamental underpinnings of epithelial tissue physiology[4]. Such scarcity of therapies urges the need for developing more clinically relevant models of epithelial tissue that facilitate studying of the respiratory system and drug screening[5].

Current research relies on either animal models or *in-vitro* transwell plate setups which mimic epithelial tissue structure and function. The latter has the advantages of being more economical, easier to implement in many laboratories, and better experimental consistency (compared to animals, which introduce variations in many tissue parameters)[6,7]. The most common *in-vitro* approach is the use of commercially available semipermeable hanging film for creating an ALI in transwell flasks[8,9]. With this technique, the film is exposed to a liquid environment on one side and air on the other. The basal side provides moisture and growth medium, while the apical side provides exposure to air, thus mimicking airway epithelial tissue. The cell culture is then grown on the air side of the film, which still contains sufficient moisture (made available via diffusion from the liquid side) for supporting cellular growth. Despite mimicking the ALI condition, conventional transwell platforms have a number of limitations. These include their relative high cost, lack of proper distribution of nutrients and waste removal due to their static conditions, prolonged culture times (average 3 weeks) required for full cell differentiation,

[a.] *School of Electrical and Computer Engineering, Purdue University, West Lafayette, IN, 47907, USA. E-mail: bziaie@purdue.edu; Tel: +1 765-494-0725.*
[b.] *Birck Nanotechnology Center, Purdue University, West Lafayette, IN, 47907, USA.*
[c.] *Division of Immunology, School of Life Sciences, Faculty of Medicine & Health Sciences, Queen's Medical Centre, University of Nottingham, Nottingham NG7 2UH, UK*
[d.] *Indiana University School of Medicine, Division of Plastic Surgery, IN, USA*
[e.] *Biomaterials Innovation Research Center, Division of Biomedical Engineering, Department of Medicine, Brigham and Women's Hospital, Harvard Medical School, Cambridge, MA 02139, USA*
[f.] *Harvard-MIT Health Sciences and Technology, Cambridge, MA, USA*
[g.] *Department of Bioindustrial Technologies, College of Animal Bioscience and Technology, Konkuk University, Seoul 143-701, Republic of Korea*
[h.] *Department of Physics, King Abdulaziz University, Jeddah 21569, Saudi Arabia*

and their inability to faithfully recapitulate the mechanics of epithelial tissue (i.e., most films are too brittle, impermeable to gases, and incompatible with microfluidic systems) [10,11]. Thus, there is a need for more cost effective, easy to use, and physiologically relevant (e.g. highly permeable for gas exchange and yet robust enough to support cell culture in liquid environment) ALI platforms[12].

As a more cost-effective approach, many researchers have successfully demonstrated the use of paper as an alternative material for conventional cell culture substrates (e.g., polystyrene, and PDMS)[13–16]. Paper is an attractive substrate for cell culture applications due to its naturally biocompatible 3D cellulose fiber composition and its webbed architecture for efficient cell attachment[17,18]. However, the inherent hydrophilic nature and low mechanical strength, when moistened, prevents its prolonged use in aqueous environments[19]. Nevertheless, impregnating the paper with hydrophobic materials (e.g., wax, silicone) can resolve some of the abovementioned shortcomings (i.e., improve mechanical strength in aqueous environments) [14]. Such hydrophobic films (e.g., wax and PDMS), printed using inkjet or screen printing, form water-repelling barriers on paper substrates; these patterns create hydrophobic-hydrophilic structures which can replace existing cell culture plates. For example, wax printing was used by Whitesides group to generate a 3D, multilayer, paper-based assay for monitoring molecular and genetic response of different cells to oxygen and nutrition gradients[20]. Wang et al. reported the use of PDMS-stamped multi-wells on paper as biomaterial scaffold for direct differentiation of human induced pluripotent stem cells (iPSCs) into functional beating cardiac tissues[21].

In this work, we further expand the capabilities of paper-based cell-culture platforms by taking advantage of silicone-coated commercial hydrophobic papers (parchment paper) as the starting material to generate desired hydrophilic patterns, amenable to controlled cell attachment, using a CO_2 laser scrubbing process, Fig. 1(b). The hydrophilic patterns also regulate the permeability of both oxygen and nutrition through the hydrophobic paper.

Experimental section

Materials, fabrication, and characterization methods

To compare different substrates for the paper-based airway model, we characterized several common hydrophobic papers and films in terms of their change in surface properties after laser treatment, wet strength (standard tensile strain tests as a function of wetting duration), and nutrition/gas permeability. These films were parchment paper (PP) (Reynolds®, Parchment Paper, 55 µm thick), wax paper (WP) (Reynolds®, Wax Paper, 30 µm thick), filer paper (FP) (Watman®, cellulose grade 1, 180 µm thick), polydimethylsiloxane (PDMS) (Sylgard 184, Dow Corning®), and a paper-PDMS (P/PDMS) composite prepared by placing a sheet of filter paper on a thin layer (50 µm) of PDMS pre-polymer spin-coated onto a silanized silicon wafer and cured at 80°C for 30 min. The performance of the papers were compared with the commercial polyethylene terephthalate (PET) transwell ALI culture membranes with 0.4 µm pore size (Corning®). The micro structural properties of the papers were compared by SEM imaging (supplementary information Fig. S1).

Previous studies have shown that the change in surface wettability with plasma and laser treatment often affects cell growth on different substrates. This method has been widely studied with different cells on various materials such as silk and polymers[22–24]. Therefore, as the first step, the surface properties of the films were characterized before and after laser treatment (at 10 W power with a scanning speed of 35 mm/s). The adjusted laser parameters were sufficient to change the surface properties of the films without completely cutting through the material. The surface wettability of samples were evaluated by measuring the static contact angle of a 10 µl droplet of DI water before and after laser treatment using an optical contact angle measuring device (Rame-Hart goniometer, model 590). All experiments were conducted five times and the mean contact angle was calculated. High magnification surface and cross-sectional scanning electron microscopy (SEM) images were also obtained to assess the change in surface morphology before and after laser ablation.

A standard tensile stress-strain test was used to characterize how well the fibers in different hydrophobic papers hold

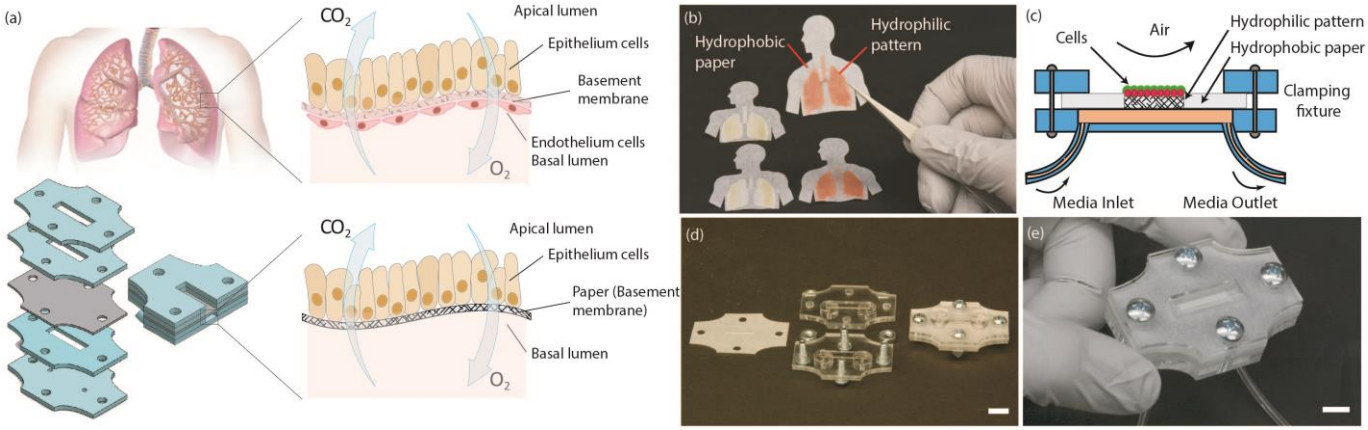

Fig. 1. (a) Illustration of the respiratory epithelial tissue and paper-based microfabricated *in-vitro* lung device, (b) selective attachment of aqueous red dye on laser treated parchment paper, (c) schematic of the paper-based air-liquid-interface (ALI) platform, (d) photograph of components, and (e) assembled final device. All scale bars: 10 mm.

together when the paper is wetted/soaked for various times. In this test, the papers were submerged in buffer saline solution (PBS) for several durations (0-7 days), and the ultimate tensile strength (UTS) and Young's modulus were subsequently measured using a universal testing machine (Admet®, model eXpert 1000). All specimens were laser cut to the same dimensions (5 mm × 20 mm). The tensile strength measurements were performed by fixing the two ends of the film and stretching from 0 % to 12 % strain at a constant extension velocity of 10 mm/min.

A customized setup was used to measure the gas permeability and oxygenation of the liquid medium through different films. The structure consisted of a cylindrical chamber filled with 20 mL of deoxygenated DI water and covered by 20 mm-diameter circular sample of the film. For all tests, the dissolved oxygen was removed by purging the water for 8 h with nitrogen gas. The oxygen permeability was confirmed with real-time measurements of the dissolved oxygen using an optical oxygen sensor (NeoFox, OceanOptics, Dunedin, FL) positioned in the DI water chamber. All measurements were performed at room temperature and atmospheric pressure. We evaluated the oxygen permeability of different membranes via the rate of dissolved oxygen increase in the water.

The permeability of cell culture media through different substrates was assessed using a conductivity measurement setup. The setup consisted of two chambers filled with 20 mL of DI water and 20 mL of growth medium (Cell, P311-500) separated by the testing membrane. The conductivity of the chamber with DI water was measured using an LCR meter at 1 kHz (GW Instek LCR-819) for 24 h. For all measurements the initial conductivity of the DI water was close to zero (1.25×10^{-6} S). The conductivity increased with time as a result of the diffusion of the ions from the medium to the DI water chamber (the receptor media), a schematic of the setup is shown in Fig. S2.

Paper-based microfluidic ALI platform

A schematic of the *in-vitro* microfluidic airway system is shown in Fig. 1(c). It consists of an upper and a lower laser-cut acrylic chamber (with 1.5 mm deep and 15 mm long channels) corresponding to the apical (airway lumen) and basal compartments of airway epithelium. The laser-treated paper provides support for cell attachment and diffusion of the fluid media to the cells. Fig. 1(d, e) show the assembling process of the platform and the final device. The device can be easily disassembled and reloaded with a new paper/film membrane for multiple experiments. In order to develop the air liquid interface model for respiratory system, the CALU3 cells (American Type Culture Collection, HTB55), was used in our experiment, which has been extensively used in *in-vitro* studies focused on the functions of bronchial airway epithelium such as tight junction formation (Zona Occluden1), mucin secretion (MU5AC) and cilia formation (β tubulin)[10,25–27].

Before assembling the ALI platform for *in-vitro* experiments, each component was ultraviolet (UV) sterilized at a distance of 8 cm for 15 min on each side. The appropriate length of inlet-outlet tubing was connected to the platform after sterilization with 70% ethanol. Upper and lower chambers were sterilized with 5x antibiotic/antimycotic solution (Sigma-Aldrich) overnight at room temperature inside the tissue culture hood. The sterilizing solution was removed and the chambers and tubing were washed with PBS.

For cell culture, the paper substrates were coated with fibronectin (10 µg/ml) (Sigma) for 1hr and then conditioned with cell culture media for 1hr before cell seeding to facilitate cell attachment. CALU-3 cells, were seeded in upper open chamber at a density of 2×10^5 cell in 200 µl of media and the whole assembly was incubated at 37 °C, 5% CO_2 for 5hrs. The bottom chamber was then infused with media at a flow rate of 8 µl/min using a syringe pump (Harvard Apparatus). The amount of media in collecting reservoir was checked every day for ensuring constant flow rate through the platform. On Day3 the cells exhibit a confluent monolayer coverage on the hydrophilic regions on the paper (5 mm x 15 mm). Next, an air-liquid interface is established for further differentiation by removing some of the medium from the top chamber while maintain the same constant flow of medium in the lower chamber for 7 days. The schematic procedure used of the ALI cell culture process is shown in Fig. S3.

Given the importance of barrier formation in epithelium integrity and its relevance to drug delivery, allergen exposure and respiratory infection, we assessed barrier formation at air liquid interface on the paper based platform by quantifying the expression of Zona Occluden1 (ZO1), a key tight junction protein, commonly used as a surrogate for quantifying for barrier formation[4,28,29,25,30]. All results were compared with conventional static ALI transwell flasks. For conventional transwell ALI cultures, 12 well format transwells from Corning® with 0.4 µm pore size were used as described before [4]. Same number of CALU-3 cells (2×10^5 cells in 200 µl) were seeded in both systems.

For immunostaining, cells were fixed with 4% paraformaldehyde and permeabilized with 0.5% Triton X-100. Then the samples were blocked with 10% goat serum (Sigma-Aldrich) for 30 min and incubated with primary antibody rabbit ZO1 (Invitrogen, UK) for 1 hour at room temperature in 1:50 dilution. Secondary antibody- goat anti rabbit Alexa fluor 488 was allowed to conjugate for an hour at room temperature. Cell nuclei were counterstained with DAPI for 15 minutes. All images are taken with Zeiss LSM710 confocal under 40x oil objective (SLIM imaging, University of Nottingham, UK).

Results and discussion

Surface wettability and morphology

The initial contact angle (CA) of the four surfaces (PP, WP, P/PDMS and PDMS) were measured to be 121°, 108°, 112°, and 94°, respectively. The P/PDMS and PDMS showed an increase in the contact angle following laser-treatment (to 115° and 126°, respectively), Fig. 2(a,b). This increase can be explained by the Wenzel theory, which predicts a higher CA for water droplets on rough hydrophobic surfaces in contrast to homogeneous surfaces (both P/PDMS and PDMS become rougher after laser treatment) [31]. In contrast, the commercial PP and WP papers

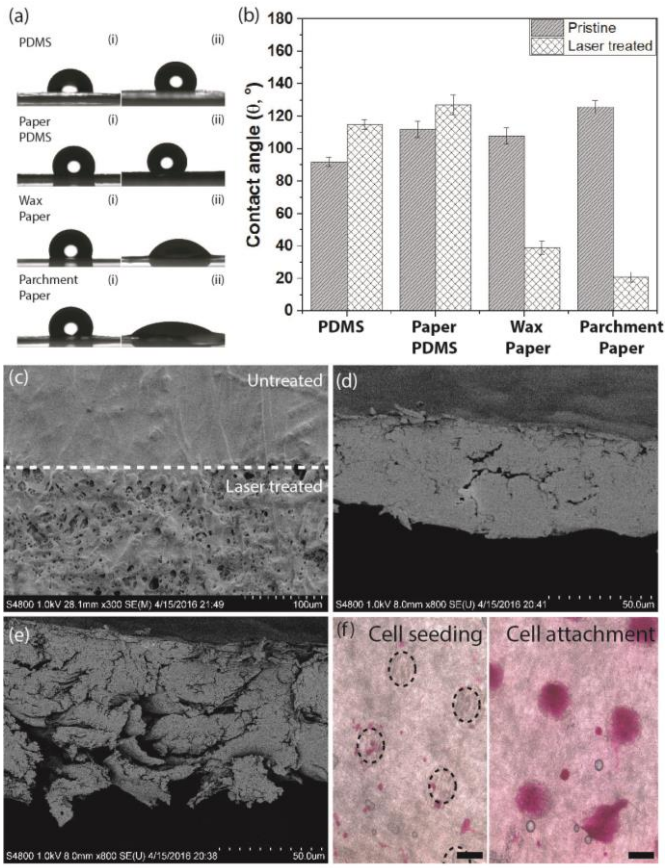

Fig.2. (a) Water droplet on different surfaces (i) before and (ii) after laser ablation, (b) comparison of contact angle of various hydrophobic surface before and after laser treatment, (c) SEM top-view of selective laser treated and untreated parchment paper, cross-section SEM image of (d) before and (e) after laser treatment of parchment paper, (f) selective cell attachment to circular hydrophilic patterns with 2mm diameter, Scale: 2 mm.

showed a significant decrease in CA to 21° and 39°, respectively, Fig. 2(a,b). This increase in surface wettability is due to the creation of exposed micro/nano cellulose fibers and addition of hydrophilic –OH, =O groups on the laser-ablated areas[32]. Fig. 2(c) shows a high magnification SEM image of selective laser-ablated parchment paper. The image show a clear change in morphology with exposed micro/nano fibers on the surface of the paper after laser treatment. The thickness of the paper was measured by cross-sectional SEM images before and after laser ablation, Fig. 2(d, e). While the initial thickness of the paper is 60 µm, the laser-ablated region was protruded out of the plane by 15 µm over the original surface. This is due to the decomposition/re-deposition of the silicone coating in the paper upon laser exposure, leading to the generation of higher-volume porous micro/nano roughness. Fig. 2(f) shows an example of how control cells attach to hydrophilic regions (2 mm diameter circles) and proliferate over time.

Mechanical properties

Fig. 3(a) shows the change in UTS for filter paper and various other hydrophobic papers/films before and after submersion in PBS. All the samples in dry states showed a linear stress-strain profile with a small strain (2.5 %) before rupture, Fig. S4. In dry state the commercial PET transwell membrane had the highest UTS with 187 MPa followed by the commercial parchment and wax papers with the UTSs of 124 MPa and 129 MPa, respectively. Filter paper impregnated with PDMS had a dry UTS of 21.4 MPa, which is three time higher than the pristine filter paper (7.6 MPa). This increase in mechanical strength was explained by the presence of the PDMS filler in the network fiber of the paper forming a stronger composite film. Wet tensile strength results, for all the paper-based specimens, showed an increase in the elasticity and a decrease in the mechanical strength.

Unlike the PET membrane that retained a stable UTS, the wet papers showed a decrease in their mechanical strength. This was due to the diffusion and plasticizing effect of water molecules in the paper films. The results show that the hydrophobic papers retained some of their mechanical strength after 24 h submerging in PBS, whereas the wet filter paper UTS drastically decreased to 1.1 MPa and started to disintegrate in the solution. Among the investigated hydrophobic papers, parchment paper retained more than 48 % of its original dry UTS strength followed by PDMS/paper and wax paper with retentions of 31% and 14 %. The parchment and wax papers showed a stable retention of mechanical strength (UTS) of 58 MPa and 11 MPa for 7 days. For filter paper and PDMS/paper, a longer wetting duration reduced the mechanical strength (UTS) down to 0.4 MPa and 5.4 MPa.

Oxygen and medium permeability

Fig. 3(b) shows the gas permeability results for different films using the aforementioned setup (inset). For all measurements the initial dissolved oxygen of the DI water was

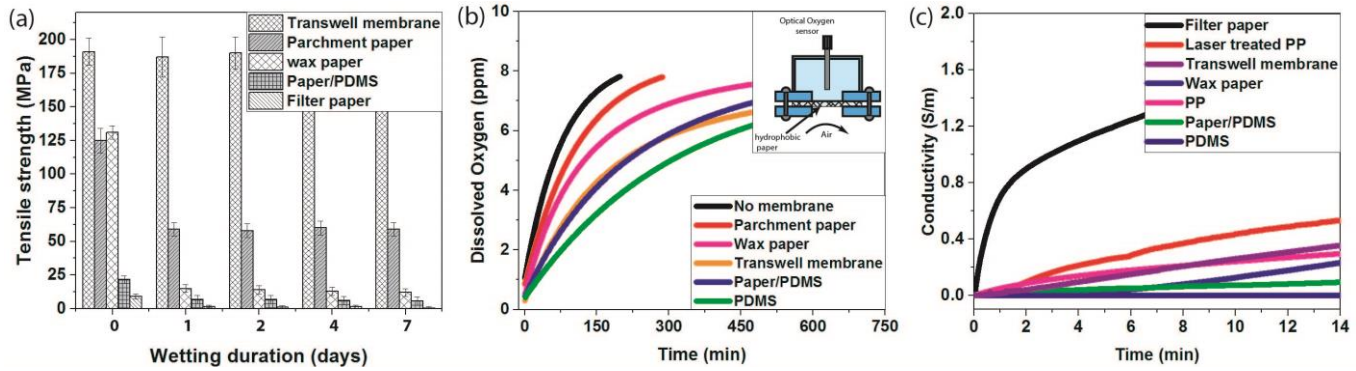

Fig. 3. (a) Ultimate tensile strength for different papers as a function of wetting duration up to 7 days, (b) oxygen permeability and dissolution in water for different hydrophobic paper membranes as function of time, the inset in (b) shows a schematic of the oxygen permeability test setup, (c) diffusion of media across various hydrophobic films as a function of time.

close to zero (~0.5 ppm) and increased with time up to the oxygen saturation level in the water (8 ppm). The increase was due to the diffusion of the oxygen gas in ambient condition through the membrane and its dissolution in the water. Without any membrane, the water equilibrates to its steady-state saturation level of about 8 ppm in less than 140 min. However, when the chamber was covered, the time required for oxygen saturation increases. The results showed the longest oxygen equilibration time occurred for a pristine 100 µm membrane of PDMS (720 min). The transwell membrane and PDMS/paper showed a similar oxygen permeability results with an average time of 650 min to oxygen equilibration. Parchment paper had a 3 fold larger oxygen permeability (time to saturation of 210 min, with an average rate of 2.4 ppm/h) as compared to the commercial transwell membrane. No signs of water leakage were observed with the hydrophobic films during any of the measurements. The mechanical strength and gas permeability results showed the superior performance of the parchment paper, providing a suitable substrate for the proposed ALI platform. Furthermore, although in the described study the cell-culture was preform on only one side of the paper (with the basal surface of the cells attached to the paper and in contact with the liquid medium, and the apical expose to air), this platform is not limited to only such setups. A more complex pulmonary *in-vitro* system, for example, might feature a co-culture environment with epithelial cells and microvascular endothelial cells on the opposite sides of the cell culture membrane, which requires gas exchange with the cells in the basal lumen. Therefore the gas permeability characterization results further show that the presented system can also be easily used for co-culture *in-vitro* pulmonary studies.

Fig. 3(c) shows the diffusion of medium across the different papers and change in electrolytic conductivity of the receptor media (starting with low conductivity DI water). The pristine hydrophilic filter paper showed the fastest change in electrolytic conductivity (1.75 S/m after 14 h). This sharp increase was due to immediate transmission of ions and media through the filter paper. The hydrophobic films (PDMS, P/PDMS, WP, PP) showed significantly smaller changes of 0.001 S/m, 0.075 S/m, 0.31 S/m, and 0.32 S/m, respectively. The low permeability of media through the hydrophobic films was due to the low permeability of wax and silicone to water and various ions present in the media[17]. The commercial PET transwell membrane also showed relatively low permeability, 0.335 S/m after 14 h with a linear increase rate of 0.023S/mh. Laser-treated PP showed a 75% increase in the permeability (0.55 S/m after 14 h, with an average rate of 0.04S/mh) as compared to an untreated sample, this was due to the porosity induced by the laser treatment, Fig2 (e).

Airway epithelial cells on the paper platform

Fig. 4 shows the cell viability on parchment paper stained by live-dead reduced biohazard cell viability assay (L7013-Life technologies) at Day1 and Day3 of cell seeding. The assay was performed according to the manufacturer's instruction. After staining, ALI platform was disassembled and the cells on parchment paper were mounted for confocal microscopy. As seen in Fig. 4, >90% of cells was viable on parchment paper at both Day1 and Day3 culture proving the compatibility of parchment paper to airway epithelium culture.

Fig.5 compares the barrier formation of airway epithelium between paper-based ALI platform under flow condition and conventional ALI method under stasis condition. The cells were stained for one of the tight junction proteins called Zonula occludens (ZO1) which was expressed as chicken wire appearance on cell membrane [33,25]. The comparison was made at two time points Day5 and Day7 of ALI culture.

Unlike cells grown on transwell membranes that showed a patchy staining for ZO-1, we observed mature thick ZO1 expression (chicken wire appearance) around the whole cell membrane on day 7 ALI culture of epithelia cells grown on parchment paper under flow resembling the functional airway epithelium. On transwell system, it take about at least 3 weeks to one month to achieve the formation of mature ZO1 expression in chicken wire appearance[25,26]. Regarding thickness of ZO1 expression, parchment paper ALI platform showed 1.19 µm ± 0.29 thickness of ZO1 at Day7 of the ALI culture whereas transwell presented 0.7µm ± 0.17 thickness. Moreover we excluded the potential influence of fibronectin coating on ZO1 formation by comparing ZO1 expression in fibronectin coated or un-coated meberanes in transwell system. These experiments showed no additional effect of fibronectin on ZO1 expression at Day 5 and Day 7 of ALI culture (Fig. S5).

In addition, we also compared the ZO1 expression between flow and static condition of the paper platform after Days 5 and 7 of ALI culture. Only small number of cells express ZO1 in immature form in static condition compared to flow condition showing the importance of the flow in air liquid interface model (Fig. S6). Collectively, paper based ALI platform induced airway epithelium to form more efficient tight junctions under flow condition.

We suggest that the parchment paper ALI chip provides a valuable tool for cost and time efficient culture for respiratory system studies under physiologically relevant conditions. The relative small surface area, the speed in which cells can form tight junction, and the ability to perform experiments under flow are highly advantageous particularly when testing drugs uptake with different flow rates and working with small number

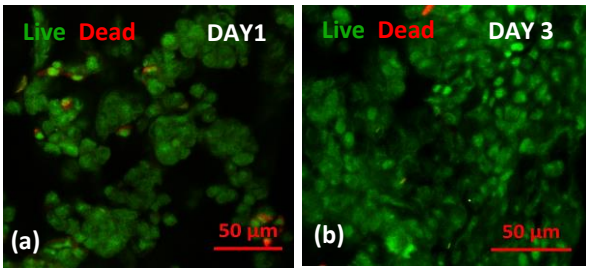

Fig. 4. Assessment of cell viability of airway epithelium (CALU3) grown on parchment paper at day1 (a) and Day3 (b) by live-dead staining. CALU3 are stained with Syto10 (Live staining- green) and Ethidium Bromide (Dead staining- red). The images were captured using Zeiss LSM710 confocal microscope under 20x objectives. (scale bar= 50 µm, 20x objective)

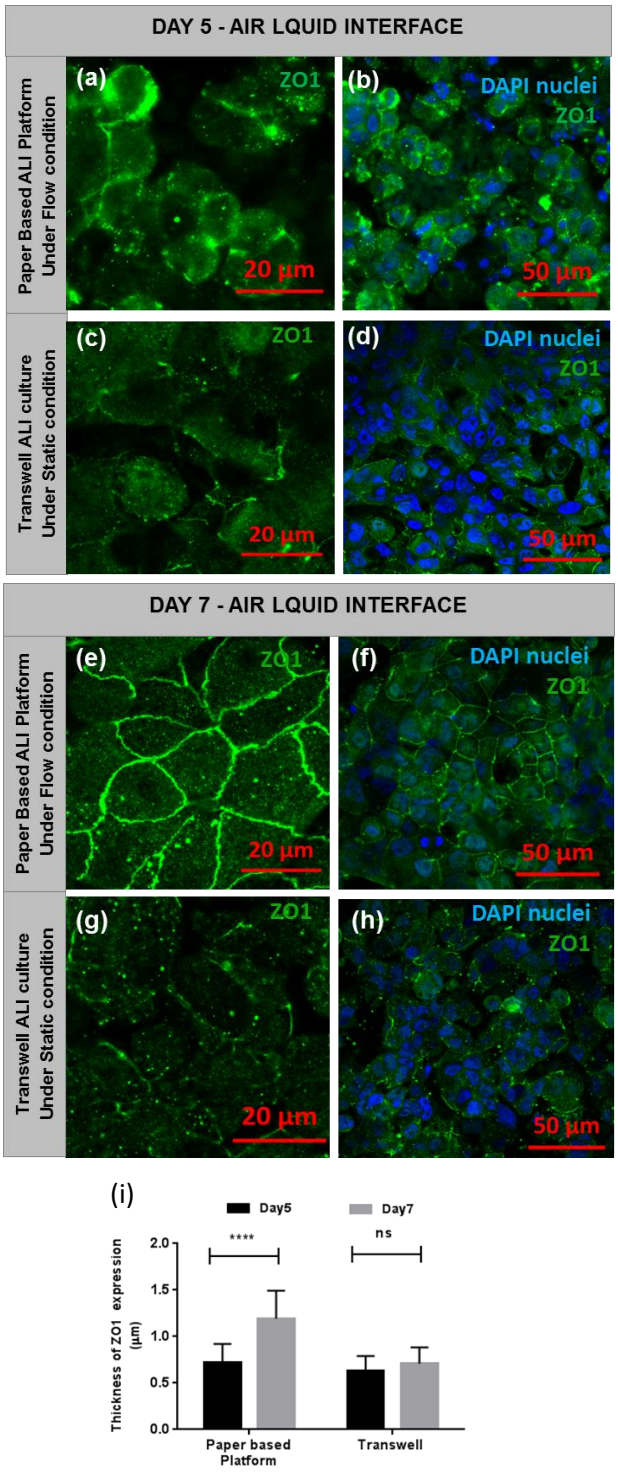

Fig. 5. Comparison of airway epithelium integrity between paper-based ALI platform and conventional Transwell ALI. Tight junctional marker - ZO1 expression was compared between ALI platform (a,b,e,f) under flow condition and Transwell (c,d,g,h) under stasis at Day5 and Day7. The first column represents the ZO1 expression (green) at 60x magnification (scale bar = 20µm) and the second column represents the overlaid images of ZO1 (green) with DAPI nuclear staining (blue) at 40x magnification (scale bar =50µm). The images were representative from 3 set of independent experiments. (i) Comparison of thickness of ZO1 expression between paper platform and Transwell at Day5 and Day7. Thickness of ZO1 was measured at 200% zoom of original image using Image J software. Mean was calculated from 100 random measurements from images of 3 independent experiments. ****p<0.0001 and ns=not significant.

of primary cells from patient groups (e.g. COPD and asthma) where typically very small amount of biological samples are available.

Conclusions

In this study, we investigated the potential use of a paper-based microfluidic system as an *in-vitro* model for human respiratory system studies. Among different papers, parchment paper showed superior performance in terms of wet strength and gas permeability. Furthermore, by selectively treating the surface of this hydrophobic paper with a CO_2 laser, we were able to produce hydrophilic regions with effective cell attachment and to regulate fluid diffusion which can resemble the semi-permeable properties observed in basement membrane of human respiratory system. The final device, composed of parchment paper and acrylic microfluidics, was able to maintain long-term stability under constant flow of media with faster barrier formation of airway epithelium compared to conventional transwell methods. It is worth highlighting that despite being widely used as surrogate for airway epithelial cells, particularly in studies focusing on barrier formation, CALU3 cells are derived from an adenocarcinoma tumour with potential functional differences with primary epithelial cells which is a limitation of the current study. . Therefore, future experiments should focus on using normal primary bronchial and alveolar epithelial cells to assess the functionality of normal airway. Given the limited availability of such cell types we believe the small surface area of the new device provides an ideal platform for such experiments. Thus, this cost-effective platform can facilitate new drug discovery and improve the understanding of the etiology for different diseases by providing a model that better simulates the respiratory barrier at the cellular level.

Acknowledgements

The authors thank the staff of the Birck Nanotechnology Center for their support. Funding for this project was provided in part by the National Science Foundation under grant EFRI-BioFlex #1240443.

References

1 C. A. Pope, *Circulation*, 2003, **109**, 71–77.
2 W. W. Thompson, *JAMA*, 2003, **289**, 179.
3 P. a Martorana, B. Lunghi, M. Lucattelli, G. De Cunto, R. Beume and G. Lungarella, *BMC Pulm. Med.*, 2008, **8**, 17.
4 H. Harrington, P. Cato, F. Salazar, M. Wilkinson, A. Knox, J. W. Haycock, F. Rose, J. W. Aylott and A. M. Ghaemmaghami, *Mol. Pharm.*, 2014, **11**, 2082–91.
5 D. Huh, H. J. Kim, J. P. Fraser, D. E. Shea, M. Khan, A. Bahinski, G. a Hamilton and D. E. Ingber, *Nat. Protoc.*, 2013, **8**, 2135–57.

6 C. Y. Chan, P.-H. Huang, F. Guo, X. Ding, V. Kapur, J. D. Mai, P. K. Yuen and T. J. Huang, *Lab Chip*, 2013, **13**, 4697–710.

7 D. Huh, G. a Hamilton and D. E. Ingber, *Trends Cell Biol.*, 2011, **21**, 745–54.

8 P. Gangatirkar, S. Paquet-Fifield, A. Li, R. Rossi and P. Kaur, *Nat. Protoc.*, 2007, **2**, 178–86.

9 M. B. Esch, T. L. King and M. L. Shuler, *Annu. Rev. Biomed. Eng.*, 2011, **13**, 55–72.

10 Y. Zhu, A. Chidekel and T. H. Shaffer, *Crit. Care Res. Pract.*, 2010, **2010**, 1–8.

11 D. Huh, B. D. Matthews, A. Mammoto, M. Montoya-Zavala, H. Y. Hsin and D. E. Ingber, *Science (80-.).*, 2010, **328**, 1662–1668.

12 S. Kumar Mahto, J. Tenenbaum-Katan and J. Sznitman, *Scientifica (Cairo).*, 2012, **2012**, 1–12.

13 J. a Potkay, *Lab Chip*, 2014, **14**, 4122–4138.

14 K. A. Simon, K. M. Park, B. Mosadegh, A. B. Subramaniam, A. D. Mazzeo, P. M. Ngo and G. M. Whitesides, *Biomaterials*, 2014, **35**, 259–268.

15 H.-J. Park, S. J. Yu, K. Yang, Y. Jin, A.-N. Cho, J. Kim, B. Lee, H. S. Yang, S. G. Im and S.-W. Cho, *Biomaterials*, 2014, **35**, 9811–23.

16 Y. Chen, Z. Kuo and C. Cheng, *Trends Biotechnol.*, 2015, **33**, 4–9.

17 R. Derda, A. Laromaine, A. Mammoto, S. K. Y. Tang, T. Mammoto, D. E. Ingber and G. M. Whitesides, *Proc. Natl. Acad. Sci. U. S. A.*, 2009, **106**, 18457–62.

18 S. Ahmed, M. N. Bui and A. Abbas, *Biosens. Bioelectron.*, 2016, **77**, 249–263.

19 H. Juvonen, A. Määttänen, P. Laurén, P. Ihalainen, A. Urtti, M. Yliperttula and J. Peltonen, *Acta Biomater.*, 2013, **9**, 6704–6710.

20 B. Mosadegh, M. R. Lockett, K. Thu, K. A. Simon, K. Gilbert, S. Hillier, D. Newsome, H. Li, A. B. Hall, D. M. Boucher, B. K. Eustace and G. M. Whitesides, *Biomaterials*, 2015, **52**, 262–271.

21 L. Wang, C. Xu, Y. Zhu, Y. Yu, N. Sun, X. Zhang, K. Feng and J. Qin, *Lab Chip*, 2015, **15**, 4283–4290.

22 L. Jeong, I. S. Yeo, H. N. Kim, Y. Il Yoon, D. H. Jang, S. Y. Jung, B. M. Min and W. H. Park, *Int. J. Biol. Macromol.*, 2009, **44**, 222–228.

23 S. C. Jin, H. S. Baek, Y. I. Woo, M. H. Lee, J.-S. Kim, J.-C. Park, Y. H. Park, D. K. Rah, K.-H. Chung, S. J. Lee and I. H. Han, *Macromol. Res.*, 2009, **17**, 703–708.

24 V. P. Ribeiro, L. R. Almeida, A. R. Martins, I. Pashkuleva, A. P. Marques, A. S. Ribeiro, C. J. Silva, G. Bonifácio, R. a. Sousa, R. L. Reis and A. L. Oliveira, *J. Biomed. Mater. Res. Part B Appl. Biomater.*, 2015, n/a–n/a.

25 C. E. Stewart, E. E. Torr, N. H. Mohd Jamili, C. Bosquillon and I. Sayers, *J. Allergy*, 2012, **2012**, 1–11.

26 M. E. Kreft, U. D. Jerman, E. Lasič, N. Hevir-Kene, T. L. Rižner, L. Peternel and K. Kristan, *Eur. J. Pharm. Sci.*, 2015, **69**, 1–9.

27 G. E. Morris, J. C. Bridge, L. a Brace, a J. Knox, J. W. Aylott, C. E. Brightling, a M. Ghaemmaghami and F. R. a J. Rose, *Biofabrication*, 2014, **6**, 035014.

28 K. Khoufache, O. Cabaret, C. Farrugia, D. Rivollet, A. Alliot, E. Allaire, C. Cordonnier, S. Bretagne and F. Botterel, *Med. Mycol.*, 2010, **48**, 1049–1055.

29 S. Dekali, C. Gamez, T. Kortulewski, K. Blazy, P. Rat and G. Lacroix, *Toxicol. Reports*, 2014, **1**, 157–171.

30 J. L. Harcourt, M. McDonald, P. Svoboda, J. Pohl, K. Tatti and L. M. Haynes, *BMC Res. Notes*, 2016, **9**, 11.

31 J. Yong, F. Chen, Q. Yang, D. Zhang, G. Du, J. Si, F. Yun and X. Hou, *J. Phys. Chem. C*, 2013, **117**, 24907–24912.

32 G. Chitnis, Z. Ding, C.-L. Chang, C. a Savran and B. Ziaie, *Lab Chip*, 2011, **11**, 1161–5.

33 I. George, S. Vranic, S. Boland, A. Courtois and A. Baeza-Squiban, *Toxicol. Vitr.*, 2015, **29**, 51–58.